Korean J. Chem. Eng., 36(8), 1235-1242 (2019)
DOI: 10.1007/s11814-019-0305-z

pISSN: 0256-1115
eISSN: 1975-7220

In-situ hydrodeoxygenation of furfural to furans over supported Ni catalysts in aqueous solution

Ze Wang*,,†, Zhaolin Fu*,***, Weigang Lin*,**, Songgeng Li*,**, and Wenli Song*,****

*State Key Laboratory of Multi-Phase Complex Systems, Institute of Process Engineering, Chinese Academy of Sciences, Beijing 100190, China
**Sino-Danish College, University of Chinese Academy of Sciences, Beijing 100190, China
***Sinopec Research Institute of Petroleum Processing, Beijing 100083, China
(*Received 25 November 2018 • accepted 21 May 2019*)

Abstract−In-situ hydrodeoxygenation of furfural as a representative component in bio-oil was investigated in aqueous solution over supported Ni catalysts, for preparing furans as an antiknock additive. The addition of methanol, ethanol, or isopropanol was found inhibitive to coke formation at 220 °C. When using methanol as the hydrogen donor and coke inhibitor, the support in mesoporous structure with moderate acidity was more favorable to the conversion of furfural and to the formation of furans. An increased loading amount of Ni facilitated the generation of deep hydrogenated products. The conversion of furfural could hardly be changed under different methanol to water ratios, while the product distribution varied remarkably. Under optimized conditions, the summary yield of furan and 2-methylfuran reached to above 85%. On the basis of optimized reaction conditions, the in-situ hydrodeoxygenation of an eight-component synthetic bio-oil was tested, and the results verified the adaptability of the method for conversion of bio-oil.

Keywords: Furfural, 2-Methylfuran, Hydrogen Donor, Methanol, In-situ Hydrodeoxygenation

INTRODUCTION

Renewable energy is an inevitable choice due to the inescapable exhaustion of fossil fuels. Biomass is an important renewable energy source, and also the only source for renewable carbon [1]. However, the lower energy density of biomass restricts its application severely. So it is advantageous to convert biomass to liquid fuels and/or high value chemicals [2,3]. Many methods have been put forward for biomass conversion, and among them the pyrolysis of biomass is a promising one with the advantages of high liquefaction efficiency and low operating pressure [4,5]. However, the poor properties of bio-oil, such as high oxygen content (~40 wt%), high water content (15-30 wt%), low heating value (17-20 MJ/kg), and high corrosivity (pH~2-4) with instability, determine that it has to be upgraded before usage [6,7].

Several upgrading methods have been broadly investigated, such as emulsification, aqueous phase reforming, catalytic cracking, and hydrodeoxygenation (HDO) [8,9]. Among them, HDO originating from the petrochemical industry is regarded as the most effective method with high deoxygenation rate [1]. However the conventional HDO process needs a large amount of external gaseous hydrogen, causing a severe challenge for running security [10]. Moreover, this process is usually carried out at relative high temperatures (200-600 °C), leading to higher energy consumption and easier formation of coke [11]. A novel method of in-situ HDO which obtains hydrogen from hydrogen donor such as formic acid, methanol, and isopropanol provides an alternative to the upgrading of bio-oil [12, 13]. In Fisk et al.'s work, the oxygen content of a synthetic bio-oil (mixture of model compounds) is reduced from 41.4 wt% to 2.8 wt% over Pt catalysts, by in-situ HDO method using light oxygenates as hydrogen donors [14]. Xu et al. investigated the in-situ hydrogenation of some model compounds (acetone and phenol) over Raney Ni catalyst with methanol as the hydrogen donor [13]. We have also studied the in-situ HDO of phenol over supported Pd, Ru, and Pt catalysts [12,15], and obtained a high phenol conversion ~90% with a high deoxygenation degree ~80% over Pd catalyst [12]. Generally, the corresponding researches are still rather scarce, and mainly focus on the conversion of phenols over noble metal or Raney Ni catalysts.

Bio-oil is a complex mixture and furans are another important group of components [10,16]; thus, the HDO of furfural (FAL) as the model compound of furans in bio-oil are also studied, using gaseous H_2 as the hydrogen source [10,17].

In this paper, the in-situ HDO of furfural in aqueous solution over supported Ni catalyst was studied for preparing furans, since furans including furan and 2-methylfuran (2-MF) with high octane number could be used as antiknock fuel additive in gasoline [17, 18]. Herein, the coking behavior of furfural was tested first as some relevant researches mentioned [10,19]. Then, catalysts and hydrogen donors were screened, and reaction conditions were further optimized for improving the furfural conversion and the selectivity to furans. Finally, the in-situ HDO of an eight-component synthetic bio-oil was tested based on optimized reaction conditions.

†To whom correspondence should be addressed.
E-mail: wangze@ipe.ac.cn

EXPERIMENTAL SECTION

1. Catalyst Preparation

The supported Ni catalyst was used herein, because of its high hydrogenation activity and relatively low price [20,21]. It was prepared by incipient wetness impregnation method [12,22] on different supports of Al_2O_3 (Alfa Aesar, 99%), SiO_2 (Alfa Aesar, 99%), ZSM-5 (XFnano, 99%), MCM-41 (XFnano, 99%), SBA-15 (XFnano, 99%). A certain amount of $Ni(NO_3)_2{\cdot}6H_2O$ (Sinopharm, ≥98.0%) was first dissolved in deionized water with the volume equivalent to the pore volume of support. Then, the solution was impregnated on the support and aged for 10 hours at room temperature with intermittent stirring. Subsequently, it was dried at 110 °C for 5 hours and then heated from room temperature to 500 °C by 5 °C/min for calcination for 5 hours. Finally, the catalyst precursor was reduced under the atmosphere of 50 vol% H_2 and 50 vol% Ar (flow rate of 300 mL/min) at 550 °C for 2 hours (heated from room temperature by 10 °C/min).

2. Catalyst Characterization

Temperature programmed reduction by H_2 (H_2-TPR) was performed (Micromeritics AutoChem II chemisorption analyzer 2920) to identify a proper temperature for reduction of the catalyst precursor. In the test, 20-50 mg sample was loaded into a U-type quartz tube, and then the temperature was increased from 50 °C to 800 °C by 10 °C/min in the atmosphere with 10 vol% H_2 and 90 vol% Ar. X-ray diffraction (XRD, PANalytical Empyrean) was conducted in the angle (2θ) range of 5-90°, with conditions of Cu Kα radiation, 40 kV and 30 mA, to characterize the chemical phases of catalysts. The catalyst surface area and pore size was characterized by N_2 adsorption/desorption method (Micromeritics ASAP 2020 HD88), and the data were treated by BET, T-plot, BJH, HK models. Temperature programmed desorption of NH_3 (NH_3-TPD) was carried out (Micromeritics AutoChem II Chemisorption Analyzer 2920) to measure the acidity of the catalyst. In the test, the sample (20-50 mg) loaded in a U-type quartz tube was first heated to 120 °C by 10 °C/min and held for 30 minutes in He atmosphere. Thereafter, it was cooled to 50 °C in the mixed 10 vol% NH_3 and 90 vol% He atmosphere for saturation of adsorption. The sample was then heated to 100 °C and flushed by He for 1 h. It was further heated to 700 °C with the heating rate of 10 °C/min to desorb NH_3, and the NH_3 concentration was measured by thermal conductivity detector (TCD) every 1 second.

3. Experimental Process

The experiments were performed in a 100 mL autoclave made of C276 Hastelloy (Dalian Tongda Reactor Work, type CJF-0.1L). For coke formation tests, 2 g furfural and 10 g deionized water without catalysts were added into the reactor, which is generally accordant with the furfural composition in crude bio-oil [23]. After reaction, the solid residue was taken out and dried at 100 °C overnight. It was then weighted to calculate the mass of coke formation. For coke inhibition tests, additional 20 g solvent (deionized water, methanol, ethanol, isopropanol, cyclohexane, or heptane) was added into the feedstock, beyond the constant 2 g furfural and 10 g water. For catalyst screening tests, 0.5 g reduced catalyst was first loaded into the reactor and then reactants and solvents were added sequentially. The in-situ HDO of a synthetic bio-oil was also tested with 4 g catalyst. The synthetic bio-oil with 2 g furfural as reference was made up of eight components: formaldehyde (10 wt%), formic acid (4 wt%), acetic acid (10 wt%), ethanol (8 wt%), 1-hydroxy-2-propanone (4 wt%), furfural (7 wt%), phenol (17 wt%), and H_2O (35 wt%) [14,24,25]. Prior to experiment, the autoclave was flushed by N_2 for three times to purge air and pressurized with N_2 to 1 MPa. Keeping stirring at 700 rpm, the reactor was heated to 120-280 °C by 3 °C/min and held for 1-6 h. Thereafter, the autoclave was cooled in a water tank to room temperature with an average cooling rate ~10 °C/min. The initial 1 MPa of N_2 is used as internal standard for calculating the amount of gas product. All gas hydrocarbons (C1-C4) are indicated by the symbol of CH.

4. Product Analysis

Gas product was analyzed by gas chromatography (GC, Shimadzu GC-2014). Liquid product was analyzed using gas chromatography-mass spectrometer (GC-MS, Thermal Scientific ISQ) equipped with a FFAP column (30 m×0.25 mm×0.25 μm). The internal standard method was applied for quantification, and ethylene glycol (Sinopharm, ≥99%) was used as the standard substance. The oven temperature was set as follows: keep at 30 °C for 5 mins, then heat to 100 °C by 4 °C/min holding for 3 mins, and finally heat to 250 °C by 5 °C/min holding for 5 mins.

The mass balance and carbon balance, coke yield, conversion, and liquid yield, are respectively, defined as follows.

$$\Delta m, \% = \left(1 - \frac{\Sigma_i^n m_{i,\,out}}{\Sigma_i^n m_{i,\,in}}\right) \times 100 \quad (1)$$

$$\Delta C(\%) = \left(1 - \frac{\Sigma_i^n m_{C,\,i,\,out}}{m_{furfural,\,in} \times \frac{60}{96}}\right) \times 100 \quad (2)$$

$$\text{Coke}, \% = \frac{m_{coke}}{m_{furfural,\,in} \times \frac{60}{96}} \times 100 \quad (3)$$

$$\text{Conversion}, \% = \left(1 - \frac{n_{furfural,\,out}}{n_{furfural,\,in}}\right) \times 100 \quad (4)$$

$$\text{Yield (liquid)}, \% = \left(1 - \frac{n_{i,\,out}}{n_{furfural,\,in}}\right) \times 100 \quad (5)$$

where, $\Sigma_i^n m_{i,\,out}$ means total mass after reaction; $\Sigma_i^n m_{i,\,in}$ total mass introduced; $\Sigma_i^n m_{C,\,i,\,out}$ total carbon mass of all the products from furfural after reaction; $m_{furfural,\,in} \times \frac{60}{96}$ initial carbon mass of furfural; m_{coke} mass of coke solid, with the assumption that coke is made from pure carbon; $n_{furfural,\,in}$ initial mole of furfural; $n_{furfural,\,out}$ mole of furfural after reaction; $n_{i,\,out}$ mole of component i after reaction.

RESULTS AND DISCUSSION

1. Inhibition of Coke

The coking behavior from conversion of furfural was first investigated, as it was the most significant and challenging problem in HDO of bio-oil [26]. Fig. 1(a) presents the coke yields from reactions without catalyst at 120-220 °C. It can be seen that when the

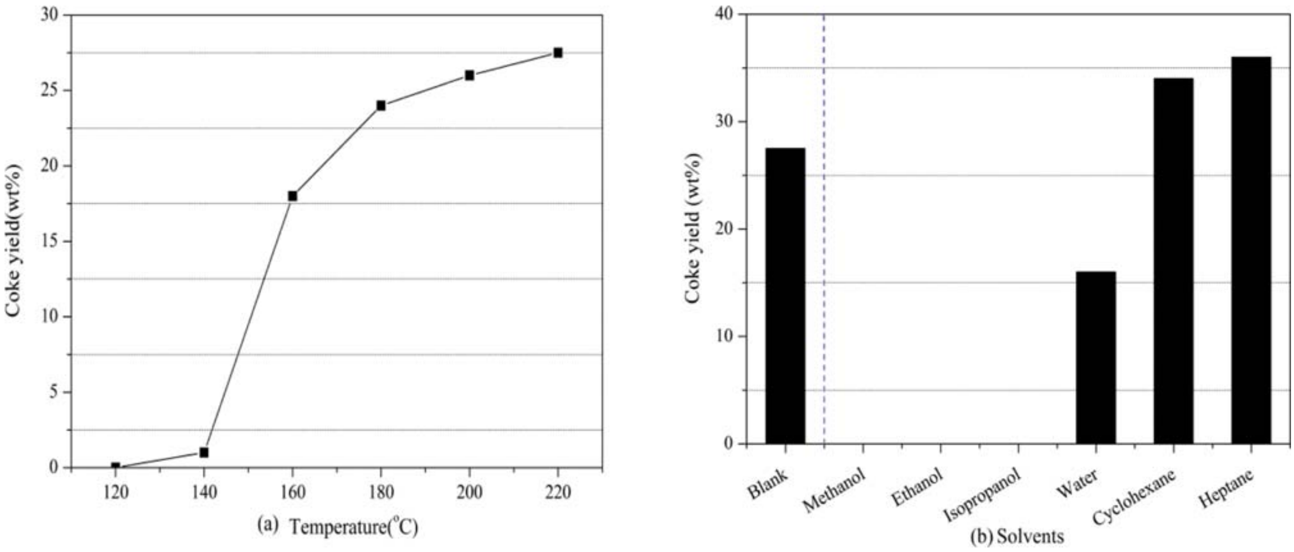

Fig. 1. Coking behavior and coke-inhibition effect by addition of solvents. Reaction conditions: furfural=2 g, H_2O=10 g, reaction time=4 h. (a) Coke yield under different temperatures without catalyst. (b) Coke yield under additional 20 g of different solvent without catalyst at 220 °C.

reaction temperature rose to 140 °C, obvious coke appeared and the coke yield got a sharp increase from ~1% at 140 °C to ~18% at 160 °C and finally to ~28% at 220 °C. When 0.5 g 5 wt% Ni/Al_2O_3 was added into the system with the temperature of 220 °C, even more coke was generated (yield of 30%) and almost no liquid product was detected by GC-MS, indicating that the catalyst was covered by coke and completely deactivated before it could play roles. The coke could be derived from self-condensation and/or polymerization of furfural and would inevitably deteriorate the whole process [27, 28]. A high temperature as well as protons from ionization of water at high temperatures was promotive to the coking process [29]. Therefore, how to effectively inhibit the coke formation was of great importance for HDO of furfural or bio-oil.

Considering that the precursor of coke could be dissolved and diluted by organic solvents and thus might prevent the combination of precursor molecules to form coke, some organic solvents were tested. The coke yields are shown in Fig. 1(b). It was found that methanol, ethanol, and isopropanol performed best for inhibiting the formation of coke, since no coke could be detected in the three systems. More water could partially inhibit the coke formation as well, but cyclohexane and heptane caused severe coking rather than inhibition. With respect to the higher hydrogen productivity and low price of methanol [30], methanol was used as both of coke inhibitor and hydrogen donor in the following experiments. A blank experiment showed that if methanol was added into the feedstock with no catalyst, almost no furfural was converted, and no gas or liquid product or coke could be detected at 220 °C, confirming the inertness of the reactor material.

2. In-situ HDO of Furfural

Repetitive experiments at 220 °C using 5 wt% Ni/Al_2O_3 as cata-

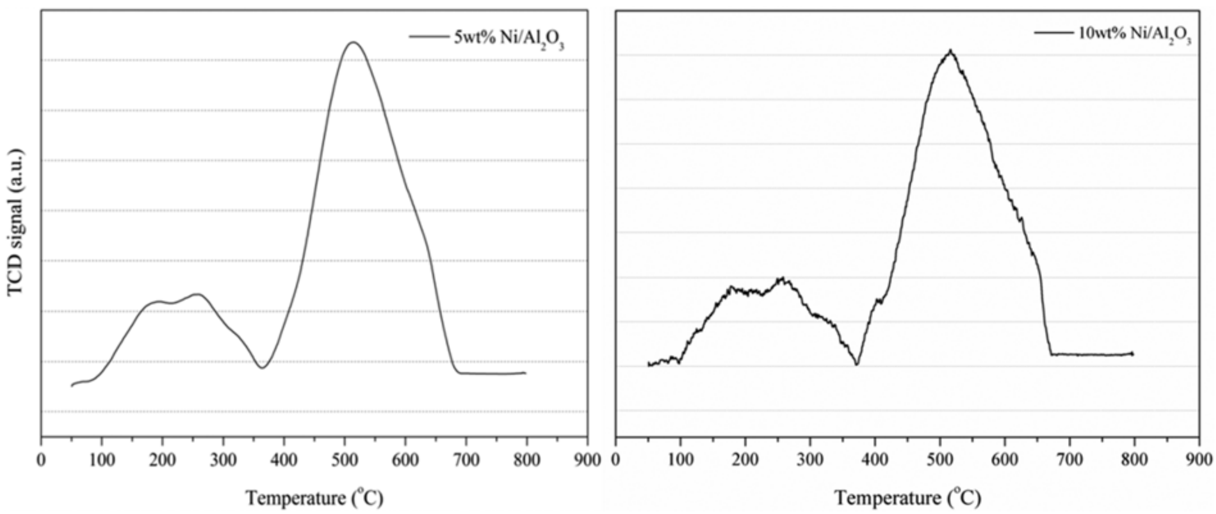

Fig. 2. H_2-TPR analysis for the catalyst precursor of 5 wt% and 10 wt%Ni/Al_2O_3.

lyst illustrated that the relative standard deviation (RSD) of furfural conversion was no higher than 4%. The mass balance and carbon balance for all experiments in this work were less than 10% deviation, indicating the qualified reliability of the experimental system.

2-1. Catalyst Characterization

The catalyst precursor of 5 wt% Ni/Al_2O_3 before reduction treatment was analyzed by H_2-TPR as shown in Fig. 2. The first-stage reduction happened in the range from 100 °C to 380 °C, which could be attributed to the reduction of the remaining $Ni(NO_3)_2$ after calcination [31]. Another wide reduction peak appeared in the range of 380-680 °C, which indicated the reduction of bulk NiO to Ni. Though the end of the reduction finished at 680 °C, the reduction treatment of the catalyst could still be completed at 550 °C by prolonging the reduction time to 2 hours [17], since the strongest peak appeared at 525 °C. An overly high temperature would readily lead to aggregation of particles and therefore deteriorate the catalyst activity. The practical and the theoretical hydrogen consumption were calculated and the difference was no higher than 10%, ensuring the relative high reduction degree.

To evaluate the influence of Ni loading on the temperature of reduction, another catalyst precursor with higher loading amount of Ni (10 wt%Ni/Al_2O_3) was also analyzed by H_2-TPR method, as shown in Fig. 2. There is no remarkable difference between the curves of 5 wt% Ni/Al_2O_3 and 10 wt% Ni/Al_2O_3, They both have two broad peaks with similar peak positions at around 250 °C and 525 °C respectively. It indicates that the loading amount of Ni did not exert significant influence on the reduction of catalyst precursor, which is accordant with the result that reported by some other researchers [32].

XRD analysis of Ni/Al_2O_3 with different Ni loading amounts is presented in Fig. 3. It can be seen that the pure Al_2O_3 had three main peaks at 37.6° (311), 45.8° (400) and 67.0° (440), with some other weak peaks [17]. Ni had three characteristic peaks appearing at 44.5° (111), 51.6° (200) and 76.4° (220) [13]. Though the first peak of Ni (111) overlapped with the Al_2O_3 (400) peak, an increasing tendency of the peak intensity could still be observed with the increase of the Ni loading amount. Likewise, the other peaks of Ni

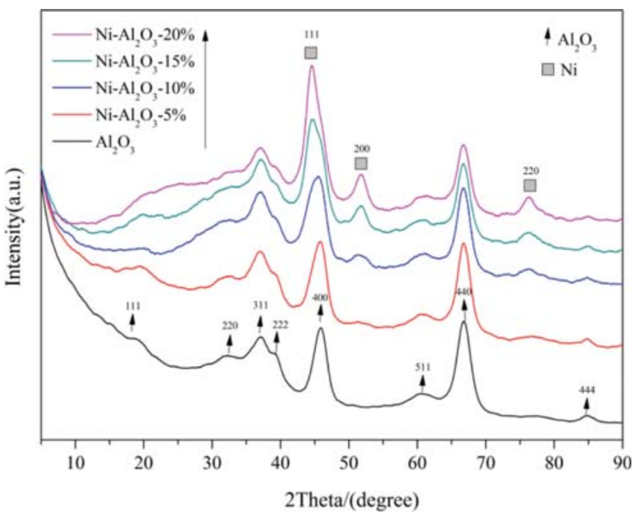

Fig. 3. XRD analysis for Ni/Al_2O_3 with different Ni loading amounts.

Table 1. Surface area and pore size of Ni/Al_2O_3 with different loading amounts of Ni

Catalyst	S_{BET} (m^2/g)	S_{Micro}[a] (m^2/g)	$S_{External}$[b] (m^2/g)	Pore size[c] (nm)
5 wt%	192	20	172	8.0
10 wt%	176	15	161	7.8
15 wt%	165	27	138	7.3
20 wt%	110	10	100	7.0

[a]S_{Mciro}: micropore area calculated through t-Plot model
[b]$S_{External}$: external surface area calculated through t-Plot model
[c]Pore size: BJH desorption average pore diameter

Table 2. Surface area and pore size of 10 wt% Ni catalysts with different supports

Catalyst	S_{BET} (m^2/g)	S_{Micro}[a] (m^2/g)	$S_{External}$[b] (m^2/g)	Pore size[c] (nm)
Ni/Al_2O_3	176	15	161	7.8
Ni/SiO_2	109	15	94	13.1
Ni/ZSM-5	142	106	36	0.43[d]
Ni/MCM-41	767	43	724	2.7
Ni/SBA-15	629	53	576	5.8

[a]S_{Mciro}: micropore area calculated through t-Plot model
[b]$S_{External}$: external surface area calculated through t-Plot model
[c]Pore size: BJH desorption average pore diameter
[d]0.43: calculated by HK method

(200) and Ni (220) showed a similar tendency as well, confirming an effective loading of Ni.

The surface area and pore size of the catalyst varied with Ni loading amount and the type of support were listed in Table 1 and Table 2, respectively.

The result shows that the external surface area contributed the most to the total surface area, which could be ascribed to the rich mesopores of Al_2O_3. With the increase of Ni loading amount, the external surface area was occupied remarkably, while the pore size just showed a slight decrease, indicating that the pore channels were not severely blocked by Ni particles.

Table 2 shows that except for ZSM-5, all other supports were of mesoporous structure in the pore size order of Ni/SiO_2>Ni/Al_2O_3>Ni/SBA-15>Ni/MCM-41>Ni/ZSM-5. Among them, Ni/MCM-41

Table 3. NH_3-TPD analysis of the 10 wt% Ni catalysts over different supports

Catalyst	Acidity (mmol/g)			
	Weak (100-230 °C)	Moderate (230-450 °C)	Strong (>450 °C)	Total
Ni/Al_2O_3	0.292	0.677	-	0.969
Ni/SiO_2	-	0.376	-	0.376
Ni/ZSM-5	0.117	0.180	-	0.297
Ni/MCM-41	0.066	0.116	0.023	0.205
Ni/SBA-15	0.123	0.283	-	0.406

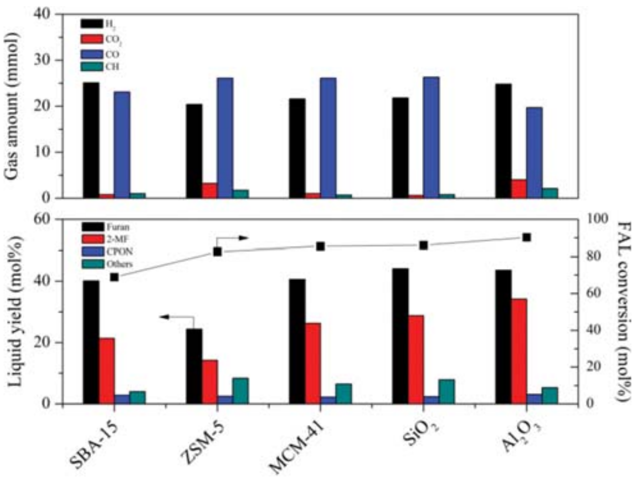

Fig. 4. Product yield and furfural conversion over 10 wt% Ni catalyst on different supports. Reaction conditions: furfural=2 g, water=10 g, methanol=36 g, reaction time=2 h, reaction temperature=260 °C. 'Others' consisted of furfuryl alcohol, cyclopentanol, tetrahydrofuran, and butanol.

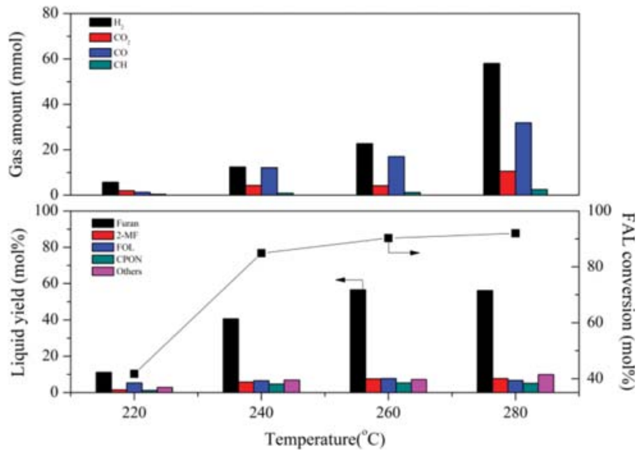

Fig. 5. Effects of reaction temperature over 5 wt% Ni/Al_2O_3 on furfural conversion and product distribution. Reaction conditions: furfural=2 g, water=10 g, methanol=18 g, reaction time=4 h. 'Others' consisted of butanol, cyclopentanol and tetrahydrofuran.

and Ni/SiO_2 had the biggest and smallest surface area, respectively.

The acidities of the catalysts with different supports were characterized by NH_3-TPD analysis, as shown in Table 3. The acid sites could be divided into three categories: the weak (100-230 °C), the moderate (230-450 °C), and the strong (>450 °C) acid sites [17]. Comparatively, the catalyst of Ni/Al_2O_3 had the most total acids and mainly moderate acidity.

2-2. Effect of Catalyst Support

The effect of catalyst support, including Al_2O_3, SiO_2, ZSM-5, MCM-41, and SBA-15, was studied. The gas and liquid yields are shown in Fig. 4. As can be seen, the support material had a very weak influence on gas product distribution, and the two components of H_2 and CO were most abundant in all systems. For liquid products, furan and 2-methylfuran were most abundant. The Al_2O_3 supported catalyst exerted the best performance on furfural conversion (90.6%) and on the summary yield of furan and 2-methylfuran (77.8%). By contrast, a lowest conversion appeared in the system with SBA-15. The catalyst with ZSM-5 gave the lowest yields of furan and 2-methylfuran due to the formation of much etherification product, which could be generated from the reaction between furfuryl alcohol and methanol. Based on the summary yield of furan and 2-methylfuran, the performances of the supports could be ranked as Al_2O_3>SiO_2>MCM-41>SBA-15>ZSM-5, indicating that a higher pore size was beneficial to the improvement of the catalyst performance.

The acidity of the support could be influential too. As Table 3 illustrates, Al_2O_3 had the most moderate acids. According to the amounts of moderate acids, the supports could be ranked as Al_2O_3>SiO_2>SBA-15>ZSM-5>MCM-41, similar to their performance ranking order. In general, a mesoporous support with larger pore size and more moderate acids like Al_2O_3 was most favorable to the conversion of furfural and to the formation of furan and 2-methylfuran, and thus Al_2O_3 was selected for further study in the following work.

2-3. Effect of Reaction Temperature

Fig. 5 illustrates the influence of temperature on furfural conversion, gas amount and liquid yield over 5 wt% Ni/Al_2O_3. The conversion of furfural increased from 41.7% to 92.0% in the range of 220 °C-280 °C, and the promoting effect of temperature was more distinct at low temperatures. For gas product, H_2 was more generated with rising temperature, from 5.7 mmol at 220 °C to 58.1 mmol at 280 °C, as the methanol conversion to H_2 was an endothermic process [33]. The amounts of other gas components increased with rising temperature as well, and particularly CO increased sharply from 1.3 mmol at 220 °C to 31.9 mmol at 280 °C. Four major products were detected in the liquid: furan, 2-methylfuran, furfuryl alcohol (FOL), and cyclopentanone (CPON). Furan, with the highest yield of 57.2% at 280 °C, was the predominant product from decarbonylation of furfural, a typical endothermic reaction [10], which was in accordance with the sharp increase of CO. The increase of temperature was generally promotive to the formation of furan and 2-methylfuran, but the product distribution became more complex, because of the appearance of some ring-opening products such as butanol and pentanediol at higher temperatures over 260 °C. Considering that there was just a slight change after 260 °C, no matter for furfural conversion or liquid product yield, 260 °C was selected as the proper temperature in the following researches.

2-4. Effect of Catalyst Metal Loading

The furfural conversion, the gas amount, and the liquid yield varied with loading amount of Ni are shown in Fig. 6. As can be seen, a higher Ni loading amount was beneficial to the conversion of methanol to give more H_2, but the undesired Fischer-Tropsch synthesis or methanation of CO was promoted simultaneously, with a remarkably augmented yield of CH, which would lead to the waste of hydrogen source. An increased Ni loading amount facilitated the conversion of furfural gently, but changed the liquid product composition distinctly. The yield of furan was reduced from 56.6% (over 5 wt% Ni/Al_2O_3) to 25.5% (over 20 wt% Ni/Al_2O_3), while more deep hydrogenated products such as tetrahydrofuran and butanol

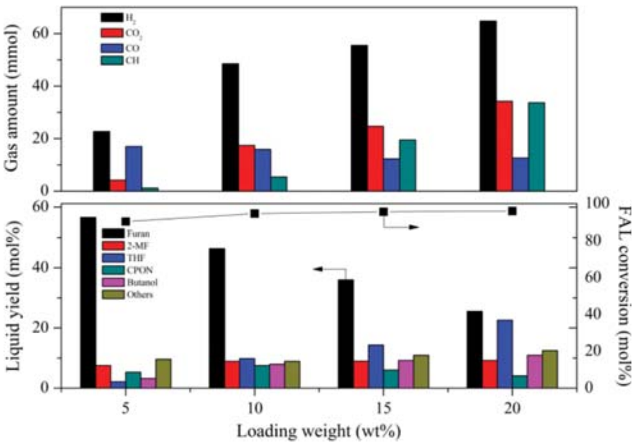

Fig. 6. Effects of metal loading over Ni/Al_2O_3 on furfural conversion and product distribution. Reaction conditions: furfural=2 g, water=10 g, methanol=18 g, reaction time=4 h, reaction temperature=260 °C. 'Others' consisted of furfuryl alcohol, cyclopentanol.

were generated, due to the increased metal sites. Therefore, Ni-based catalyst had a catalytic effect on both aldehyde group and furan ring of furfural. Considering that 10 wt% Ni/Al_2O_3 provided a higher furfural conversion with a higher yield of furan and 2-methylfuran, it was selected as the optimal loading amount of Ni and applied in the following research.

2-5. Effect of Feed Ratio

By changing the added amount of methanol, the effect of feed mole ratio of methanol to water (0.5, 1, 1.5, 2) on the conversion of furfural and on product yields was investigated, as shown in Fig. 7. For gas product, the maximum H_2 amount appeared at a ratio of 1 : 1, which is consistent with the reported result that the proper mole ratio of methanol to water was around 0.8-1.0 for maximizing the yield of hydrogen [34,35].

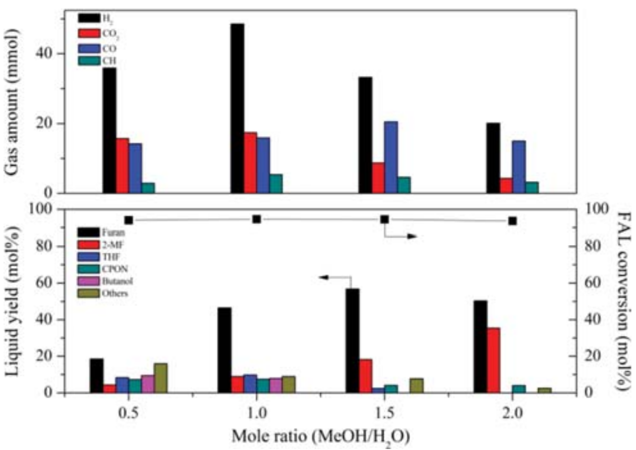

Fig. 7. Effect of methanol to water ratio on furfural conversion and product distribution over 10 wt% Ni/Al_2O_3. Reaction conditions: furfural (FAL)=2 g, water=10 g, reaction time=4 h, reaction temperature=260 °C. 'Others' consisted of furfuryl alcohol, cyclopentanol.

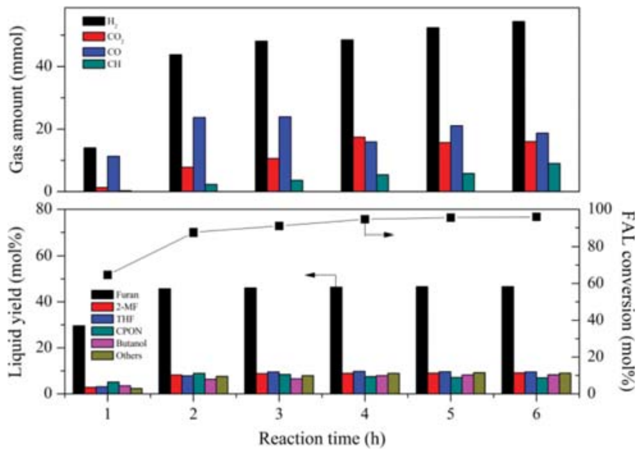

Fig. 8. Effects of reaction time on furfural conversion and product distribution over 10 wt% Ni/Al_2O_3. Reaction conditions: furfural=2 g, water=10 g, methanol=18 g, reaction temperature=260 °C. 'Others' consisted of furfuryl alcohol, cyclopentanol.

As for liquid, the conversion of furfural generally remained constant under varied methanol-to-water ratios, while the product distribution changed remarkably. The yield of 2-methylfuran distinctly increased with rising methanol-to-water ratio, and the highest value of 36.4% was achieved at the highest ratio of 2 : 1. Additionally, the summary yield of furan and 2-methylfuran accounted for 86.7% of the total liquid product at the methanol-to-water ratio of 2 : 1, while the corresponding hydrogen yield was the lowest, indicating a high efficiency of hydrogen utilization. Beyond the utilization of the generated H_2 gas, the hydrogenation and the hydrogenolysis reactions may also occur through hydrogen radicals as well, due to the initial existence of methanol rather than gaseous H_2 [36].

2-6. Effect of Reaction Time

The influence of reaction time was studied as shown in Fig. 8. The gas amount and liquid yield as well as the conversion of furfural changed faster before 2 hours, and then the changes became much slower. Comparatively, the variation extent of gas product was relatively higher than that of liquid product after 2 hours, indicating that the reactions such as methanol reformation and F-T synthesis proceeded continuously thereafter. For liquid products, the primary decarbonylation of furfural to furan was generally completed in 2 hours, which was consistent with other reports [17,37]. However, as time went on, some minor reactions such as the formation of tetrahydrofuran (from 7.8 mol% after 2 hours to 9.5 mol% after 6 hours) from furan ring hydrogenation and butanol (from 6.3 mol% after 2 hours to 8.3 mol% after 6 hours) from ring opening reaction could still proceed slowly.

3. Mechanism Discussion

The reaction mechanism was speculated as follows. Methanol worked as a hydrogen donor in this system. It adsorbed on the metal sites first, and then decomposed to CO and H_2 and/or H radical, which would participate in following hydrogenation and/or hydrogenolysis of furfural. Additionally, the water-gas shift reaction, methanation of CO, and F-T synthesis reactions might happen in the system to generate CO_2 and light hydrocarbons. The carbon atom in the aldehyde group of furfural adsorbed on Ni sites, while

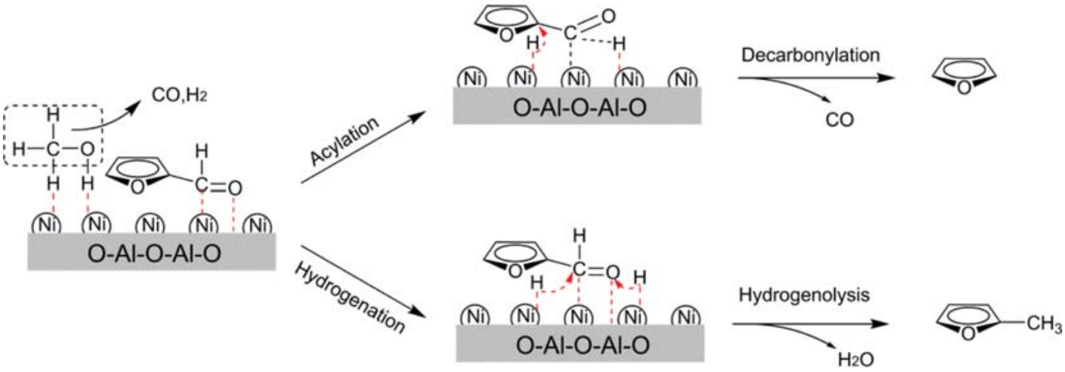

Fig. 9. Reaction mechanism for furfural to furan and 2-methylfuran with methanol as hydrogen donor over Ni/Al_2O_3.

the oxygen atom of the aldehyde mainly adsorbed on acid sites of the support as illustrated in Fig. 9. If the carbon atom on the ring structure linked with carbonyl group was attacked by H atom, the decarbonylation product of furan and CO would be obtained. If the adsorbed carbon and oxygen atom in carbonyl group was both attacked by H atom, alcohol would be generated, and would further convert to 2-methylfuran by hydrogenolysis.

4. In-situ HDO of Synthetic Bio-oil

In-situ HDO of an eight-component synthetic bio-oil over 4 g 10 wt% Ni/Al_2O_3 was tested at 260 °C for 4 h with the addition of 36 g methanol. The amount of gas components was: CH: 31.1 mmol, H_2: 20.0 mmol, CO: 14.2 mmol, CO_2: 35.0 mmol. The liquid product composition is shown in Table 4 (the components with peak area percentages less than 1% were neglected). As can be seen, formaldehyde and formic acid disappeared completely. Combined with the much generated H_2, CO, CO_2, CH in gas product, it could be deduced that the small oxygenates like formaldehyde and formic acid were readily converted to gas products. Acetic acid got a sharp decrease and simultaneously a large amount of methyl acetate was generated from esterification of acetic acid with methanol, which was beneficial for reducing the acidity of bio-oil. The component of 1-hydroxy-2-propanone was largely transferred to propanone by hydrogenolysis of hydroxyl group under Ni/Al_2O_3 catalyst. The content of ethanol did not change obviously just with 10 mol% ethanol methyl ether yield, which would not exert negative influence to the quality of bio-oil.

As to the conversion of furfural, the generation of tetrahydrofuran and 2-methylfuran from conversion of furfural was much improved while the formation of furan was inhibited, compared with that from conversion of a single furfural. The reason could partially be attributed to the additional generation of H_2 from conversion of formic acid and formaldehyde, and also may be partially attributed to the interactions and competitive adsorptions of the components.

Phenol was highly effectively converted to benzene, cyclohexanone, cyclohexanol, and cyclohexane, demonstrating that the catalyst of Ni/Al_2O_3 and the corresponding reaction conditions could be adapted to the upgrading of bio-oil through the in-situ HDO process without gaseous hydrogen addition.

To estimate whether cokes were remarkably generated on the catalyst surface, the catalyst 10 wt%Ni/Al_2O_3 after reaction was dried and weighed, for comparison with the mass of fresh catalyst before usage. Seen from the outside, there was no obvious change of the catalyst surface after reaction. The mass deviation of the catalyst before and after usage was 3.25%, which indicated that no severe coking happened on the catalyst surface during reaction.

Table 4. The components of synthetic bio-oil before and after conversion

Synthetic bio-oil	Conversion (mol%)	Upgraded bio-oil	Yield (mol%)
Formaldehyde	100	-	-
Formic acid	100	-	-
Acetic acid	100	Methyl acetate	100
Ethanol	10	Ethanol methyl ether	10
1-Hydroxy-2-propanone	100	Propanone	95
Furfural	95	Furan	11
		Furfural alcohol	9
		Tetrahydrofuran	5
		2-Methylfuran	68
Phenol	80	Benzene	14
		Cyclohexanone	12
		Cyclohexanol	10
		Cyclohexane	36

CONCLUSION

In-situ hydrodeoxygenation of furfural, as a representative component in bio-oil, was investigated. It was found that when the reaction temperature was higher than 140 °C, obvious coke would be generated from the condensation or polymerization reaction of furfural, while the addition of methanol, ethanol or isopropanol could effectively inhibit the coke formation. The support of Al_2O_3 in large pore size with high percentage of moderate acids favored the conversion of furfural and the formation of furan and 2-methylfuran. A high reaction temperature or a high Ni loading amount in Ni/Al_2O_3 was beneficial to the conversion of furfural, but was accompanied with a more complex product distribution, attributed to the occurence of more reactions. The methanol-to-water ratio exerted a very weak influence on the conversion of furfural but had a strong impact on product distribution, which could be reflected by the much generated 2-methylfuran. The decarbonylation of furfural to furan was generally completed in 2 hours, while a longer time was necessary for deep hydrogenation reactions. The in-situ HDO of an eight-component synthetic bio-oil over Ni/Al_2O_3 was tested at 260 °C for 4 h with the addition of methanol, and the results confirmed the adaptation of the method in upgrading of bio-oil without gaseous hydrogen addition.

ACKNOWLEDGEMENTS

This work was supported by the National Natural Science Foundation of China (51476180), and the National Key R&D Program of China (2018YFB0605000). Specially, thanks Anker Degn Jensen for discussions and suggestions.

SUPPORTING INFORMATION

Additional information as noted in the text. This information is available via the Internet at http://www.springer.com/chemistry/journal/11814.

REFERENCES

1. G. W. Huber, S. Iborra and A. Corma, *Chem. Rev.*, **106**, 4044 (2006).
2. S. N. Naik, V. V. Goud, P. K. Rout and A. K. Dalai, *Renew. Sust. Energy Rev.*, **14**, 578 (2010).
3. P. S. Nigam and A. Singh, *Prog. Energy Combust.*, **37**, 52 (2011).
4. J. C. Serrano-Ruiz and J. A. Dumesic, *Energy Environ. Sci.*, **4**, 83 (2011).
5. J. S. Kim, *Bioresour. Technol.*, **178**, 90 (2015).
6. T.-S. Kim, S. Oh, J.-Y. Kim, I.-G. Choi and J. W. Choi, *Energy*, **68**, 437 (2014).
7. H. Wang, J. Male and Y. Wang, *ACS Catal.*, **3**, 1047 (2013).
8. Z. Yang, A. Kumar and R. L. Huhnke, *Renew. Sust. Energy Rev.*, **50**, 859 (2015).
9. Q. Bu, H. Lei, A. H. Zacher, L. Wang, S. Ren, J. Liang, Y. Wei, Y. Liu, J. Tang, Q. Zhang and R. Ruan, *Bioresour. Technol.*, **124**, 470 (2012).
10. K. Yan, G. Wu, T. Lafleur and C. Jarvis, *Renew. Sust. Energy Rev.*, **38**, 663 (2014).
11. D. C. Elliott, *Energy Fuels*, **21**, 1792 (2007).
12. Y. Zeng, Z. Wang, W. Lin, W. Song, J. M. Christensen and A. D. Jensen, *Catal. Commun.*, **82**, 46 (2016).
13. Y. Xu, J. Long, Q. Liu, Y. Li, C. Wang, Q. Zhang, W. Lv, X. Zhang, S. Qiu, T. Wang and L. Ma, *Energy Convers. Manage.*, **89**, 188 (2015).
14. C. A. Fisk, T. Morgan, Y. Ji, M. Crocker, C. Crofcheck and S. A. Lewis, *Appl. Catal. A-Gen.*, **358**, 150 (2009).
15. Y. Zeng, Z. Wang, W. Lin and W. Song, *Chem. Eng. J.*, **320**, 55 (2017).
16. Z. Tang, Q. Lv, Y. Zhang, X. F. Zhu and Q. X. Guo, *Ind. Eng. Chem. Res.*, **48**, 6923 (2009).
17. S. Bhogeswararao and D. Srinivas, *J. Catal.*, **327**, 65 (2015).
18. V. V. Pushkarev, N. Musselwhite, K. An, S. Alayoglu and G. A. Somorjai, *Nano Lett.*, **12**, 5196 (2012).
19. A. Bohre, S. Dutta, B. Saha and M. M. Abu-Omar, *ACS Sustain. Chem. Eng.*, **3**, 1263 (2015).
20. S. Sitthisa and D. E. Resasco, *Catal. Lett.*, **141**, 784 (2011).
21. X. Zhang, T. Wang, L. Ma, Q. Zhang and T. Jiang, *Bioresour. Technol.*, **127**, 306 (2013).
22. P. M. Mortensen, J.-D. Grunwaldt, P. A. Jensen and A. D. Jensen, *ACS Catal.*, **3**, 1774 (2013).
23. P. M. Mortensen, J. D. Grunwaldt, P. A. Jensen, K. G. Knudsen and A. D. Jensen, *Appl. Catal. A-Gen.*, **407**, 1 (2011).
24. T. Stedile, L. Ender, H. F. Meier, E. L. Simionatto and V. R. Wiggers, *Renew. Sust. Energy Rev.*, **50**, 92 (2015).
25. K.-K. Cheng, J.-A. Zhang, H.-Z. Ling, W.-X. Ping, W. Huang, J.-P. Ge and J.-M. Xu, *Biochem. Eng. J.*, **43**, 203 (2009).
26. X. Li, R. Gunawan, Y. Wang, W. Chaiwat, X. Hu, M. Gholizadeh, J. Bromly and C.-Z. Li, *Fuel*, **116**, 642 (2014).
27. W.-M. Xiong, Y. Fu, F.-X. Zeng and Q.-X. Guo, *Fuel Process. Technol.*, **92**, 1599 (2011).
28. Y. Li, C. Zhang, Y. Liu, X. Hou, R. Zhang and X. Tang, *Energy Fuels*, **29**, 1722 (2015).
29. F. S. Asghari and H. Yoshida, *Ind. Eng. Chem. Res.*, **45**, 2163 (2006).
30. J. Shabaker, *J. Catal.*, **215**, 344 (2003).
31. Y. Nakagawa, H. Nakazawa, H. Watanabe and K. Tomishige, *ChemCatChem*, **4**, 1791 (2012).
32. S. Zhang, L. Dong, B. Xue, J. Chen, N. Guan and F. Zhang, *React. Kinet. Catal. Lett.*, **89**, 1 (2006).
33. C. Siriruang, S. Charojrochkul and P. Toochinda, *Monatsh. Chem.*, **147**, 1143 (2016).
34. T. Y. Amiri and J. Moghaddas, *J. Fuel Chem. Technol.*, **44**, 84 (2016).
35. Y. Shi, X. Du, L. Yang, Y. Sun and Y. Yang, *Int. J. Hydrogen Energy*, **38**, 13974 (2013).
36. F. Vogel, J. L. D. Blanchard, P. A. Marrone, S. F. Rice, P. A. Webley, W. A. Peters, A. K. Smith and J. W. Tester, *J. Supercrit. Fluid*, **34**, 249 (2005).
37. N. S. Biradar, A. A. Hengne, S. N. Birajdar, R. Swami and C. V. Rode, *Org. Process Res. Dev.*, **18**, 1434 (2014).

Supporting Information

In-situ hydrodeoxygenation of furfural to furans over supported Ni catalysts in aqueous solution

Ze Wang[*,,†], Zhaolin Fu[*,***], Weigang Lin[*,**], Songgeng Li[*,**], and Wenli Song[*,**]**

*State Key Laboratory of Multi-Phase Complex Systems, Institute of Process Engineering, Chinese Academy of Sciences, Beijing 100190, China
**Sino-Danish College, University of Chinese Academy of Sciences, Beijing 100190, China
***Sinopec Research Institute of Petroleum Processing, Beijing 100083, China
(*Received 25 November 2018 • accepted 21 May 2019*)

Adsorption and desorption curves for the catalyst of Ni/Al_2O_3 with different Ni loadings:

5%Ni/ Al_2O_3:

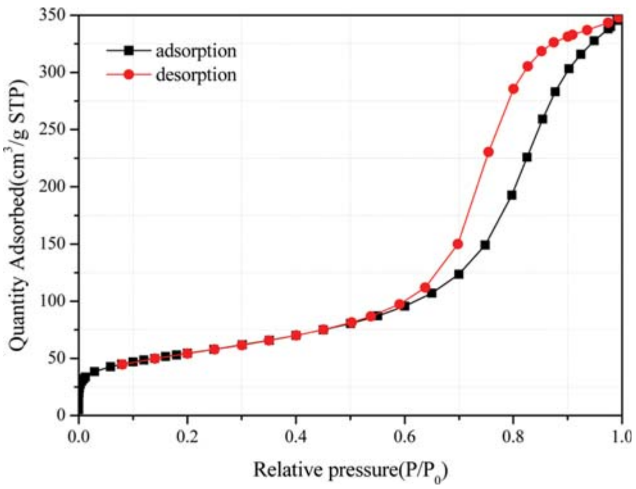

10%Ni/Al_2O_3:

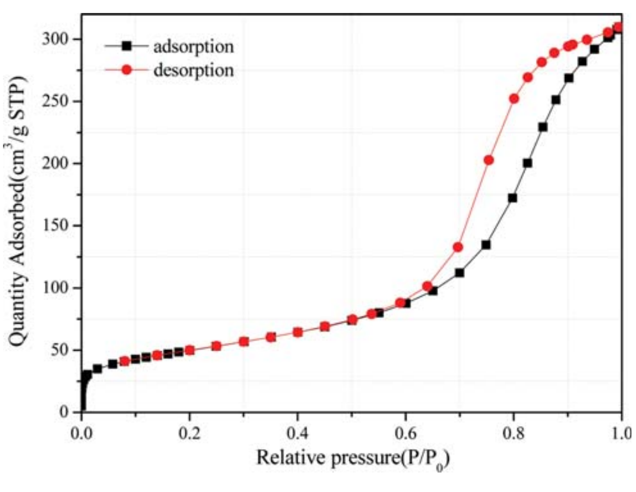

15%Ni/Al_2O_3:

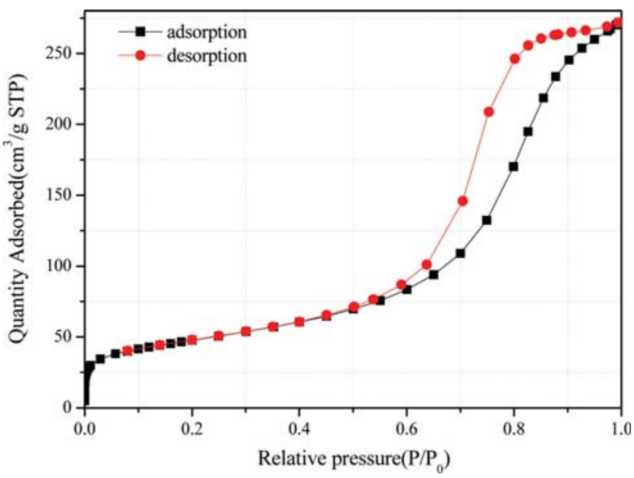

20%Ni/Al_2O_3:

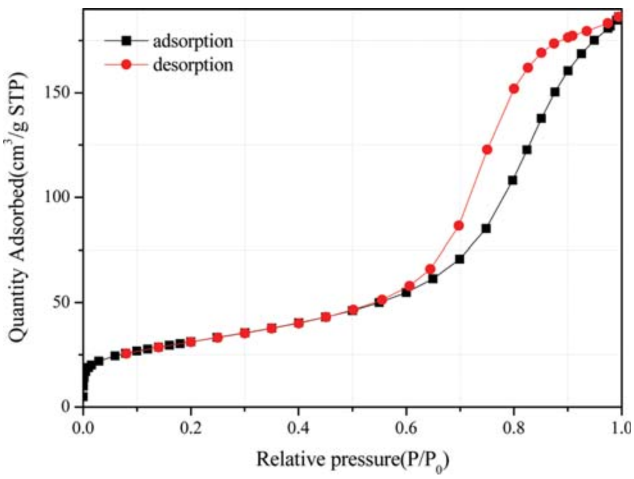

Adsorption and desorption curves for different supported catalysts with 10%Ni:

10% Ni/SiO_2:

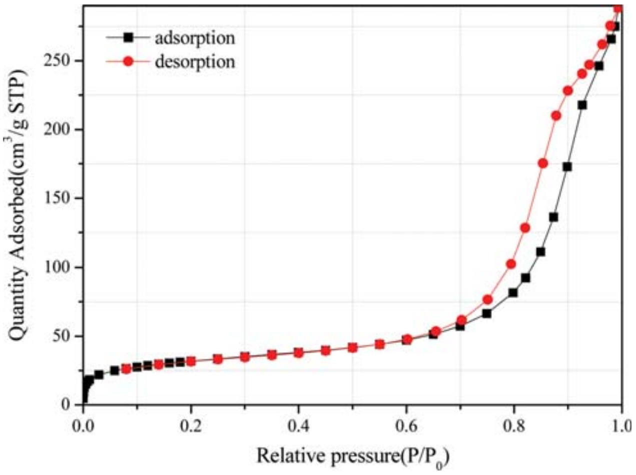

10% Ni/ZSM-5:

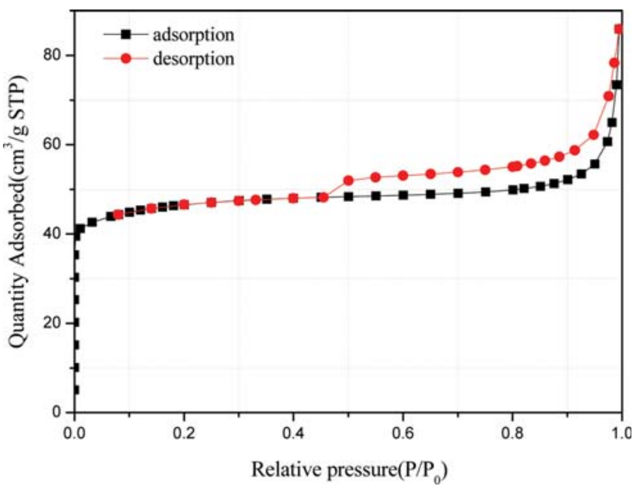

10% Ni/MCM-41:

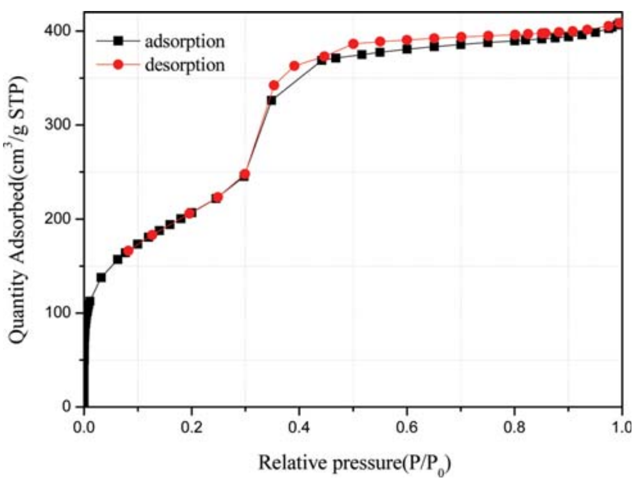

10% Ni/SBA-15:

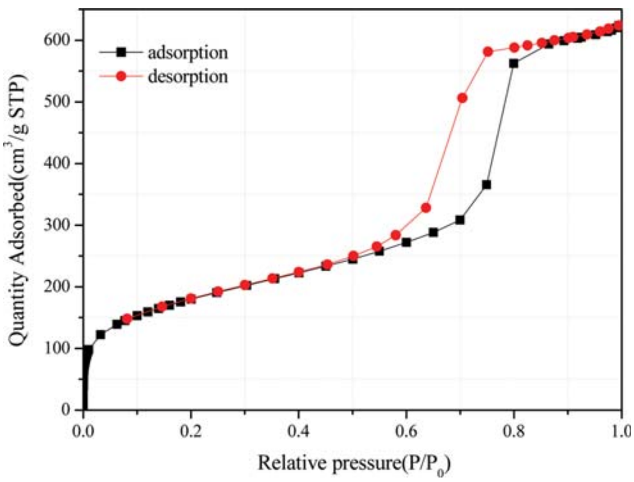

The BJH desorption pore size distributions of catalysts:

5%Ni/Al_2O_3:

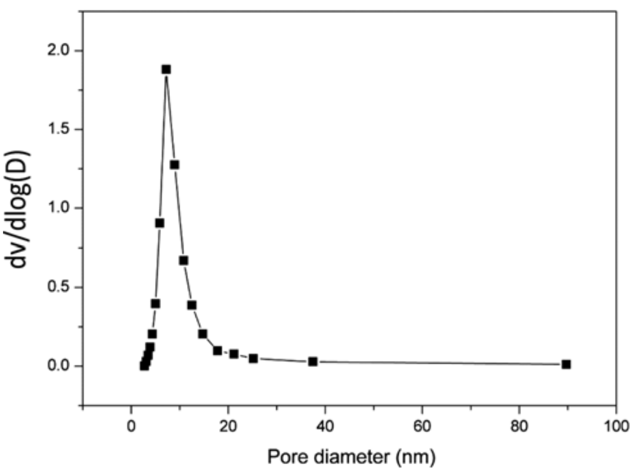

10%Ni/Al_2O_3:

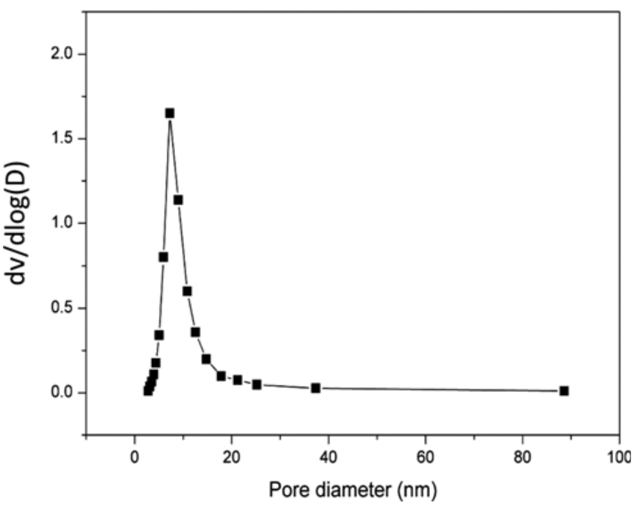

15%Ni/Al_2O_3:

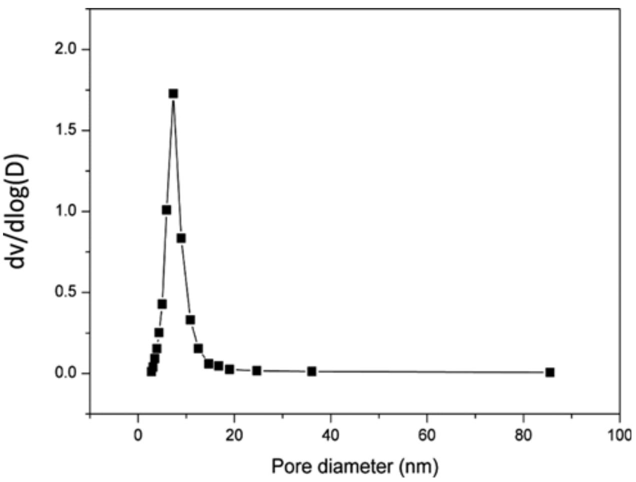

10%Ni-MCM-41:

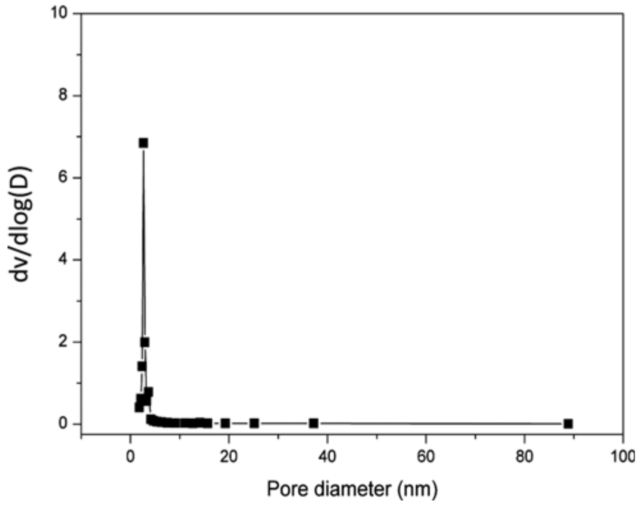

20%Ni/Al_2O_3:

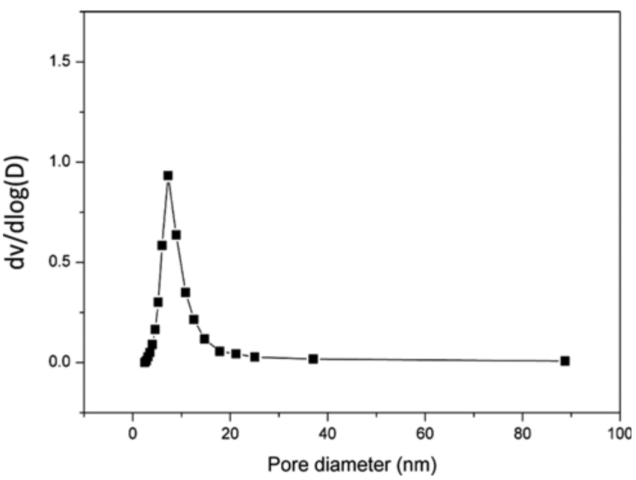

10%Ni-SBA-15:

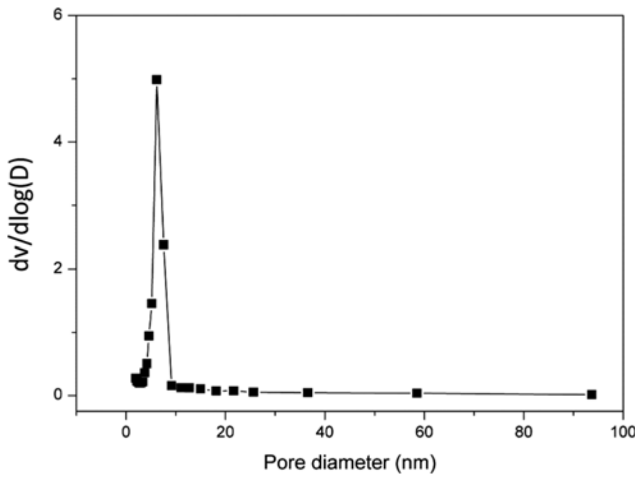

10%Ni/SiO_2:

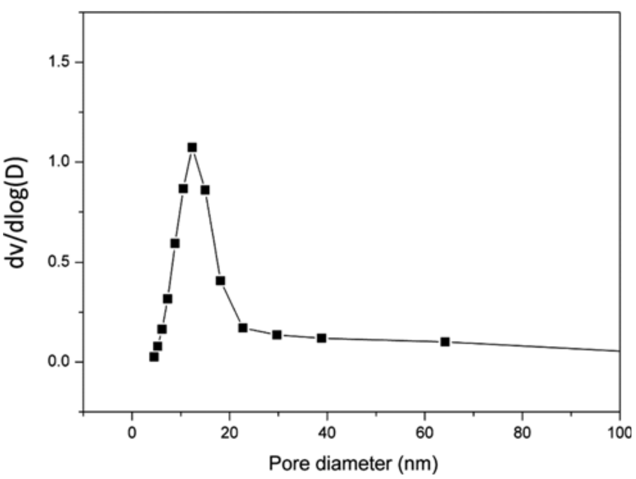

The pore size of 10%Ni-ZSM-5 calculated by Horvath-Kawazoe model:

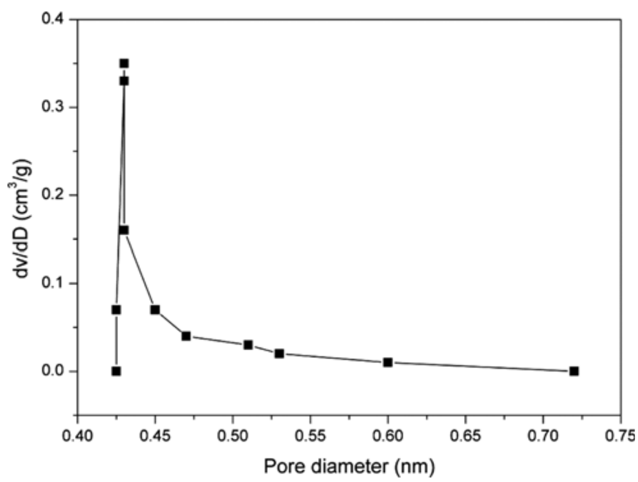

The NH3-TPD curves of catalysts:

$10\%Ni\text{-}Al_2O_3$:

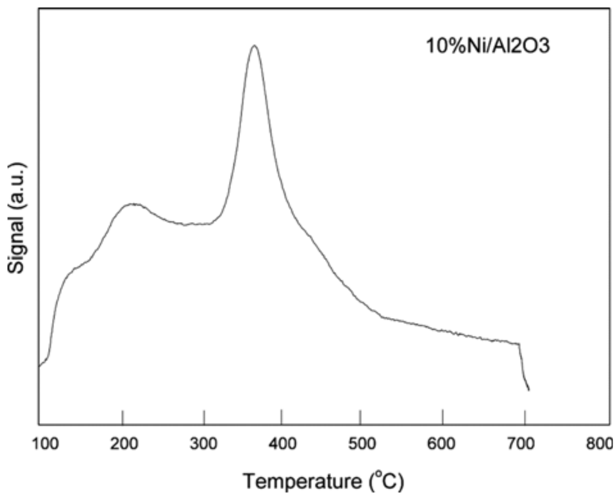

$10\%Ni\text{-}SiO_2$:

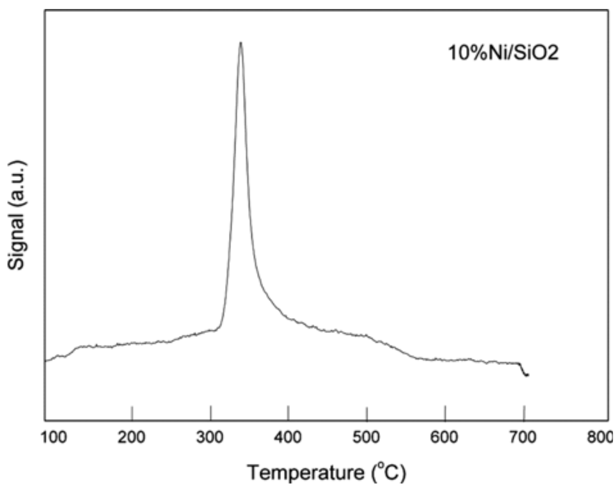

10%Ni-ZSM-5:

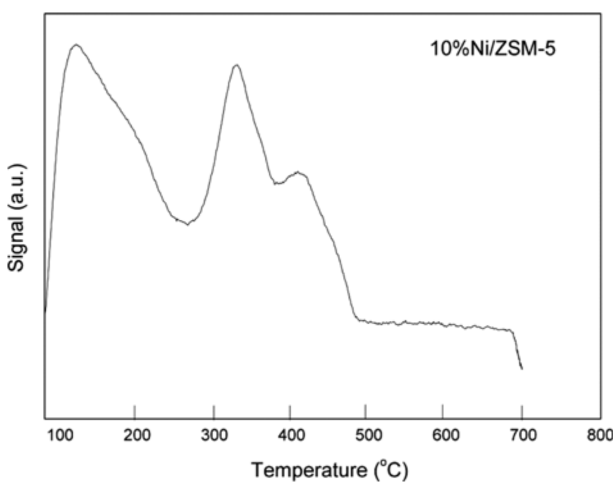

10%Ni/MCM-41:

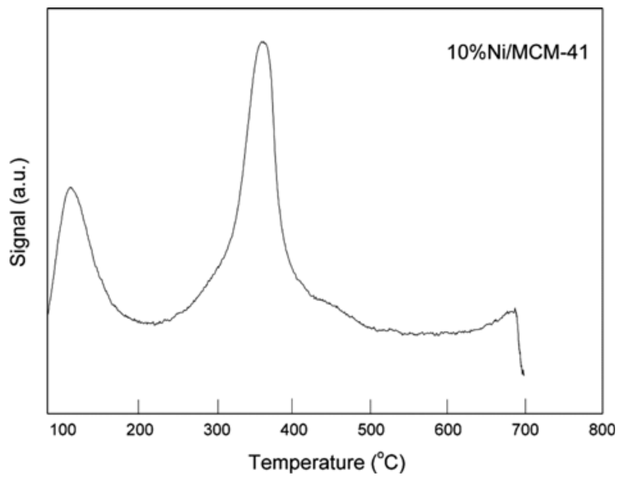

10%Ni/SBA-15: